Gas-Phase Reactions of Co^+ with Ethylamine: A Theoretical Approach to the Reaction Mechanisms of Transition Metal Ions with Primary Amines

Xiaoqing Lu,[†] Wenyue Guo,*[,†] Tianfang Yang,[†] Lianming Zhao,[†] Senchang Du,[†] Ling Wang,[†] and Honghong Shan*[,‡]

College of Physics Science and Technology, China University of Petroleum, Dongying, Shandong 257061, PR China, and College of Chemistry and Chemical Engineering, China University of Petroleum, Dongying, Shandong 257061, PR China

Received: February 25, 2008; Revised Manuscript Received: March 15, 2008

We report herein a comprehensive study of gas-phase reactions of Co^+ with ethylamine using density functional theory. Geometries and energies for all the stationary points involved in the reactions are investigated at the B3LYP/6-311++G(2df,2pd) level. Six different "classical" N and "nonclassical" ethyl-H attached isomers are found for the Co^+−ethylamine complexes. The classical complexes are much more stable than the nonclassical ones, which have the complexation energies close to Co^+ complexes with small alkanes. Extensive conversions could occur readily between these encounter complexes. All conceivable reaction pathways from each encounter complex to the experimentally observed products are carefully surveyed, and the most likely reaction mechanisms are derived. Activation of the C^{α}−H bond of ethylamine by Co^+ through both the classical and nonclassical complexes leads to not only the H_2 loss but also the hydride abstraction. The loss of ethylene arises from Co^+ insertion into the polar C−N bond in the classical complexes as well as from C^{β}−H activation through the nonclassical methyl-H attached complex of Co^+−*gauche*-ethylamine. CH_4 only forms via C−C activation from the nonclassical complex with the metal bound to two Hs from the different carbons. Initial N−H insertion is unlikely to be important. It is the reactions of the nonclassical complexes that closely parallel with the Co^+ + alkane reactions. The theoretical work sheds new light on the title reactions and can serve as a theoretical approach to the reaction mechanisms of transition metal ions with primary amines.

1. Introduction

Gas-phase reactions of "naked" transition metal ions with amines have been extensively experimentally investigated for more than two decades.[1–11] The relative extent of these reactions has been determined to depend on both the metal ions and the amines.[12,13] Fe^+ was found to be the only first-row transition metal ion that inserts into the C−N bond of *n*-$C_3H_7NH_2$.[13a,b] Earlier ion cyclotron resonance (ICR) study of Co^+ reactions with a number of primary amines reported by Radecki and Allison demonstrated some reactions such as dehydrogenation, hydride abstraction, demethanation, and loss of other hydrocarbon neutrals; and products associated with C−N activation were not observed.[14] The systematic investigation on various amines (including secondary amines and triethylamine) let the authors reach a number of conclusions on the chemistry of Co^+ with primary amines in the gas phase:[14] (1) the amine nitrogen is not a strong "direct" group for transition metal ions and amine reactions closely parallel alkane reactions; (2) formation of CoH is predominantly an α-hydride abstraction; (3) H_2 elimination occurs through Co^+ insertion into one of the N−H bonds followed by a β-H shift; (4) loss of methane and other hydrocarbon neutrals could be attributed to insertion of Co^+ into the respective C−C bond followed by a β-H shift; (5) the failure of Co^+ to insert into the R−NH_2 bond is due to the weak Co^+−NH_2 bond (bond energy was derived as <18.7 kcal/mol). Even so, several later experiments have been found to contrast with some of these points. Metastable ion (MI) spectrum reported by Chen and Miller[15] suggested that metastable dissociation of Co^+−ethylamine produces the neutrals H_2, C_2H_4, and CoH. The results are somewhat different from those of Radecki and Allison where the loss of CH_4 instead of C_2H_4 was observed.[14] The loss of C_2H_4, although absence of the alternative loss of NH_3, suggests Co^+ indeed can insert into the C−N bond of ethylamine. This is not a surprise, because the Co^+−NH_2 bond energy was reported to be as large as 60.7 kcal/mol,[16] indicating formation of intermediates for the C_2H_4 loss should be exothermic. Studies employing a number of D-labeled propylamines by Schwarz and co-workers suggested that a "remote functionalization" mechanism is involved in the loss of C_2H_4 for Ni^+ and Co^+ and of H_2 for Fe^+ and Co^+ (originated exclusively from the β and γ positions of the propyl chain),[13a] which is remarkably different from the above-mentioned initial N−H insertion mechanism where the Co^+-mediated loss of molecular hydrogen was conjectured to come from the C^{α} and N positions of primary amines.[14] In other words, in spite of the extensive experimental studies, it still remains open to address the mechanistic details of reactions of transition metal ions with primary amines.

A promising approach to unveiling these reaction mechanisms needs to combine these excellent experimental data with results of electronic structure theory. Already theory has been able to provide useful quantitative structural and energetic information for quite large, electronically complicated organometallic species.[17–25] Particularly noteworthy is the density functional theory (DFT) in its B3LYP functional.[26–30] Surprisingly, electronic structure calculations of transition ions + amines are still scarce. Recently, theoretical studies of reactions of Cu^+ with

* Correspondence should be addressed to wyguo@hdpu.edu.cn and shanhh@hdpu.edu.cn
† College of Physics Science and Technology.
‡ College of Chemistry and Chemical Engineering.

10.1021/jp801653t CCC: $40.75
Published on Web 05/10/2008

ethylenediamine and methylamine as well as Co^+ with allylamine have been accomplished by Alcamí's and our groups, and with the help of these theoretical results some new insights into the respective reactions have been gained.[31–33]

In this article, we report a comprehensive theoretical study of the Co^+ + ethylamine reactions. Ethylamine is considered as the simplest prototype of primary amines containing bonds of C−H, N−H, C−C, and C−N. Products arising from Co^+ insertion into the C−H or N−H (loss of H_2 and CoH), C−C (loss of CH_4), and C−N (loss of C_2H_4) bonds have been experimentally observed.[14,15] Thus, the reactions of ethylamine are typical for primary and secondary amines. The goal of this paper is to unravel the reaction mechanisms of Co^+ with primary amines. This includes an intact illustration of all possible ion−neutral complexes and all possible pathways associated with the observed products using density functional theory as well as a comparison of the theoretical results with the experimental findings.[14,15] We expect this work could shed some new light on the reaction mechanisms of transition-metal ions with primary amines.

2. Computational Details

The geometries of all the reactants, intermediates, and products involved in the title reactions were fully optimized using the hybrid DFT including Becke's unrestricted nonlocal three-parameter functionals[34] for the DFT exchange and the correlation from the Lee, Yang, and Parr correlation functional,[26,35] i.e., the UB3LYP method, in conjunction with the basis set of 6-311++G(2df,2pd). The performance of the B3LYP/6-311++G(2df,2pd) level was found to be sufficiently reliable when compared with the experimental results available (see Table S1 in Supporting Information). Vibrational frequencies of all the optimized species were calculated at the same level to confirm the stationary points as local minima or transition states and to obtain zero-point energies (ZPE). All energies are reported with ZPE corrections. The ZPE scaling factor was determined to be 0.946 on the basis of a least-squares fit of the B3LYP/6-311++G(2df,2pd) calculated frequencies with the experimental values of the ethylamine molecule.[36] To confirm the connection of transition states with the corresponding reactants and products for some key steps, intrinsic reaction coordinate (IRC)[37] calculations were performed. We also detected the values of $\langle S^2 \rangle$ for all the calculated species to evaluate if spin contamination can influence the quality of the results. Taking into account that in DFT the value of $\langle S^2 \rangle$ is underestimated, [38] for species with deviation of $\langle S^2 \rangle$ larger than 5%, the internal and external stabilities of the DFT solutions were detected with the help of Hermitian stability maxtrices **A** and **B**[39] and the DFT wave functions were optimized when they have any instabilities. On the basis of the optimized wave functions, the structures of the species were then reoptimized to give more reliable results. All of the calculations were carried out using the GAUSSIAN 03 program package.[40]

We also made use of the natural bond orbital (NBO) theory to characterize the bonding characters between different groups for some species involved. These calculations were performed by using the NBO5.0 program package.[41]

3. Results and Discussion

For transition metal containing systems, possible crossing between surfaces corresponding to different spins should be taken into account. We have excluded the possibility of crossing between the first excited state, the quintet state and the ground state (the triplet state) for the Co^+ + allylamine reactions previously.[32] Considering the similarity of the Co^+/amine systems, in the following only the triplet surface (the ground surface) of $[Co, N, C_2, H_7]^+$ will be discussed.

TABLE 1: Possible Products as Well as the Calculated Reaction Energies (in kcal/mol) at 0 K Associated with the H_2, CoH, CH_4, and C_2H_4 Loss in the Reactions of Co^+ with Ethylamine

products	reaction energies[a]
(**1**−**1**) $Co^+(CH_2CHNH_2) + H_2$	−36.4
(**1**−**2**) *trans*-Co^+−$NHCHCH_3 + H_2$	−43.2
(**1**−**3**) *cis*-Co^+−$NHCHCH_3 + H_2$	−42.9
(**1**−**4**) *c*-$Co^+(NHCH_2CH_2) + H_2$	0.8
(**1**−**5**) Co^+-$NCH_2CH_3 + H_2$	17.5
(**1**−**6**) Co^+−$CH_2CHNH_2 + H_2$	−39.4
(**2**−**1**) $CoH + CH_3CHNH_2^+$	−13.6
(**2**−**2**) $CoH^+ + CH_3CHNH_2$	47.2
(**3**−**1**) $Co^+CHNH_2 + CH_4$	−39.4
(**4**−**1**) $Co^+NH_3 + C_2H_4$	−43.8
(**4**−**2**) $Co^+(CH_2CH_2) + NH_3$	−10.2
(**4**−**3**) $Co^+NH_2 + C_2H_5$	19.1
(**4**−**4**) $CoNH_2 + C_2H_5^+$	70.2

[a] The B3LYP/6-311++G(2df,2pd) results.

We arrange this section according to the following order: first, we present structures of molecular reactants and encounter complexes as well as potential energy surface (PES) for conversions between these encounter complexes; then, we give the theoretical results of the H_2, CoH, CH_4, and C_2H_4 eliminations in turn, including geometries for all relevant species and PES profiles for all possible product channels; last, we make a comparison of the present theoretical results with experimental findings.[14,15] For the sake of clarity, Table 1 tabulates all possible products as well as calculated reaction energies associated with these products, and calculated total energies, zero point energies as well as $\langle S^2 \rangle$ values for all the relevant species are given as Supporting Information (see Table S2).

3.1. Molecular Reactants and Encounter Complexes. An exhaustive analysis of the ethylamine conformations has been published by Zeroka et al.[36] Two conformational isomers noted as *trans*- and *gauche*-ethylamines (*trans*- and *gauche*-**EA** in abbreviations) were identified due to different orientations of the amino group with respect to the ethyl group. In the present work, both of the isomers are also identified; the resulting structures are shown in Figure 1 together with the experimental structural parameters.[36] It can be found that agreements between the calculated and experimental results are fairly good. Moreover, the two isomers are found to be isoenergetic (see Table S2), suggesting coexistence of them in the gas phase.

All possible complexes of Co^+ with **EA** are considered and six encounter isomers, namely **1a**, **1a′**, **1b**, **1c**, **1d**, and **1d′**, are found. Optimized geometries as well as selected structural parameters for the complexes are shown in Figure 1, and fundamental information about the complexes is summarized in Table 2. These isomers correspond to direct attachments of Co^+ at different sites of the neutral ligands, divided into two groups: "classical" N attached complexes (noted as **1a**, **1a′**) and "nonclassical" ethyl-H attached complexes (**1b**, **1c**, **1d**, **1d′**) or, according to the conformations of the neutral ligands, into three groups, that is, Co^+-*gauche*-**EA** (**1a**, **1d**), Co^+-*trans*-**EA** (**1a′**, **1d′**), and complexes of Co^+ with either *gauche*- or *trans*-**EA** (**1b**, **1c**). It can be found from Table 2 that the Co^+-**EA** bond dissociation energy (BDE) of the classical complexes (∼59 kcal/mol) is about twice as large as that of the nonclassical ones (∼29 kcal/mol). Note that the BDEs of the nonclassical complexes are close to those of Co^+ complexes with small alkanes, such as ethane and propane.[42–48]

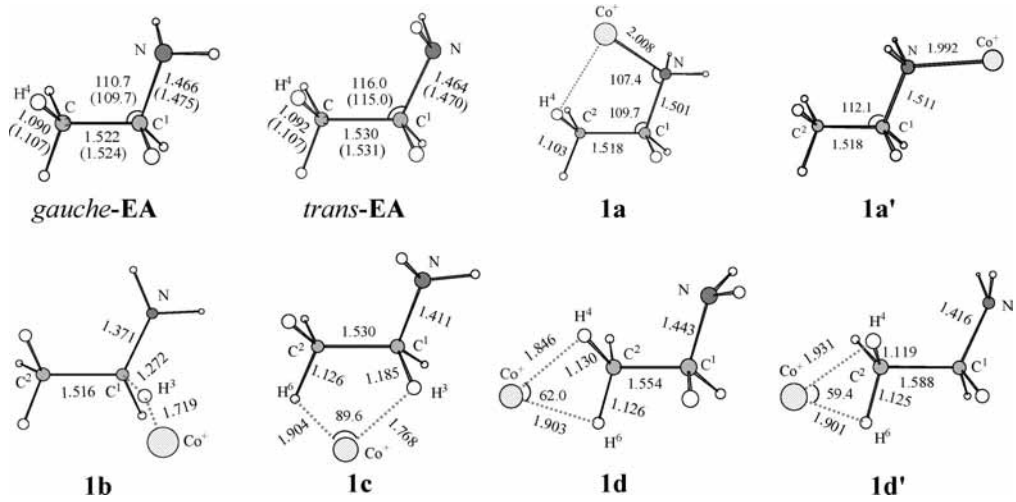

Figure 1. Geometries and selected structural parameters optimized at the B3LYP/6-311++G(2df,2pd) level for ethylamine and Co^+−ethylamine complexes. Values in the parentheses are experimental results.[36] Bond lengths are in angstroms, and bond angles are in degrees.

TABLE 2: Summary of the B3LYP/6-311++G(2df,2pd) for Calculations for Co^+−Ethylamine

					second-order perturbation theory analysis[a]	
complexes	neutral ligand	complexation site	BDE (kcal/mol)	natural charge on Co (e)[a]	orbitals involved	$E^{(2)}$ (kcal/mol)
1a	*gauche*-**EA**	N	59.8	0.841	LP(N) → 4s*(Co)	39.4
					$\sigma(C^2-H^4)$ → 4s*(Co)	3.9
1a′	*trans*-**EA**	N	58.4	0.843	LP(N) → 4s*(Co)	44.2
					$\sigma^*(N-Co)$ → $\sigma^*(C^1-H^3)$	45.3
1b	*gauche*-**EA**	η^1	29.2	0.792	$\sigma(C^1-H^3)$ → $\sigma(N-Co)$	22.2
	trans-**EA**	methylene-H			$\sigma^*(N-Co)$ → $\sigma(N-Co)$	10.8
					$\sigma(N-Co)$ → $\sigma^*(C^1-H^3)$	5.9
1c	*gauche*-**EA**	η^2			$\sigma(C^1-H^3)$ → 4s*(Co)	17.9
	trans-**EA**	methylene and methyl-Hs	30.3	0.862	$\sigma(C^2-H^6)$ → 4s*(Co)	12.0
					LP(N) → $\sigma^*(C^1-H^3)$	14.6
1d	*gauche*-**EA**	η^2 methyl-Hs	28.9	0.918	$\sigma(C^2-H^4)$ → 4s*(Co)	11.4
					$\sigma(C^2-H^6)$ → 4s*(Co)	8.9
					$\sigma(C^2-H^4)$ → 3d*(Co)	2.2
					$\sigma(C^2-H^6)$ → 3d*(Co)	2.7
					$\sigma(C^2-H^4)$ → 4s*(Co)	7.3
1d′	*trans*-**EA**	η^2	27.9	0.874	$\sigma(C^2-H^6)$ → 4s*(Co)	10.9
		methyl-Hs			$\sigma(C^2-H^4)$ → 3d*(Co)	3.9
					$\sigma(C^2-H^6)$ → 3d*(Co)	1.6

[a] The NBO//B3LYP/6-311++G(2df,2pd) results.

The classical complexes is structurally analogous to ethylamine complexes with Cu^+, Ag^+, and Na^+,[10,23] in which **1a** corresponds to Co^+-*gauche*-**EA** favored by a C_1 *cis*-Co^+−N−C−C association, and **1a′** to Co^+-*trans*-**EA** with an overall C_s *trans*-Co^+−N−C−C attachment. NBO analysis shows that both the associations are stabilized largely by electron transfer from the N lone pair into the empty metal 4s orbital (see Table 2), resulting in the stretch of the C−N bonds (R = 1.501 and 1.511 Å) as well as the shortening of the neighboring C−C bonds (R = 1.518 and 1.518 Å). Correspondingly, the Co^+-**EA** BDEs are calculated to be as large as 59.8 and 58.4 kcal/mol for **1a** and **1a′**, respectively. Note that an agostic interaction of the metal with the C−H bond parallel with the Co^+−N line (i.e., C^2-H^4) is also favored for **1a** as mirrored by the C−H bond length (1.103 Å compared to 1.090 Å in free molecule). Such a conformation provides more chances for Co^+ insertion into the C−H, C−C, and C−N bonds, which would give the corresponding products, i.e., the loss of H_2, CoH, CH_4, and C_2H_4 as observed in the gas-phase experiments.[14,15]

In addition to these classical complexes, more interestingly, there exist four nonclassical ethyl-H attached complexes. **1b** constitutes the first one, in which Co^+ attaches at one (H^3) of the methylene H's of either *gauche*- or *trans*-**EA** with a BDE of 29.2 kcal/mol. Analogous to the situation of the nonclassical association of Cu^+ with methylamine,[33] this association results in weakening of the C^1-H^3 bond as well as strengthening of the neighboring skeleton bonds, i.e., the C−C and C−N bonds. In fact, NBO analysis shows that this complex has a bonding situation strictly similar to the Cu^+ complex.[33] The other nonclassical complex with either *gauche*- or *trans*-**EA** is **1c**, in which Co^+ coordinates to two C−H bonds from the different carbon centers, accounting for the strongest "nonclassical" binding (BDE = 30.3 kcal/mol). Approach of the metal toward the methyl end of *gauche*- and *trans*-**EA** could result in the η^2 methyl-H coordinated complexes **1d** and **1d′**, respectively. These complexes are stabilized to some extent by electron donations from both the coordinated σ(C−H) bonding orbitals into the metal 4s and 3d orbitals, giving the complexation energies of 28.9 kcal/mol for **1d** and 27.9 kcal/mol for **1d′**.

As discussed above, attack of Co^+ at different base sites of **EA** could lead to different encounter complexes. Calculated PES for conversions between these complexes as well as schematic representations of the relevant structures are given in Figure 2, and information about the relevant transition states is given as

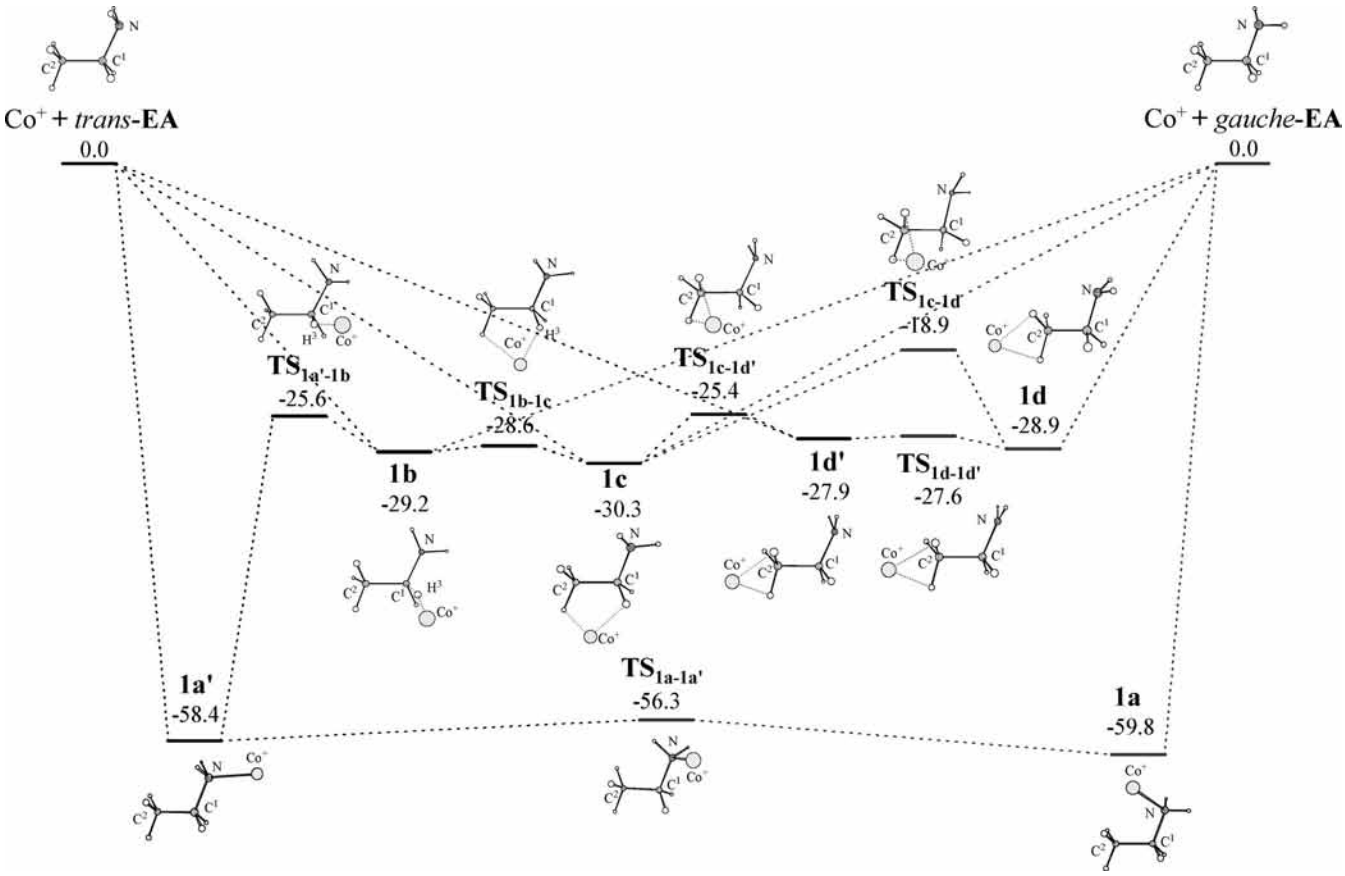

Figure 2. Energy profile for the simplest transformations between the Co^+−ethylamine complexes. Numbers refer to the relative energies with respect to the entrance channel evaluated at the B3LYP/6-311++G(2df,2pd) level including ZPE corrections. Energies are in kcal/mol.

Supporting Information (see Figure S1). It can be found that extensive conversions could take place among these encounter complexes, which can be divided into two groups: (1) transformations involving simple metal movements via transition states $\mathbf{TS_{1a'-1b}}$, $\mathbf{TS_{1b-1c}}$, $\mathbf{TS_{1c-1d}}$, and $\mathbf{TS_{1c-1d'}}$ (**1a′** ↔ **1b**, **1b** ↔ **1c**, and **1c** ↔ **1d**, **1d′**); (2) those associated with vibrations of the NH_2 group via transition state $\mathbf{TS_{1a-1a'}}$ and $\mathbf{TS_{1d-1d'}}$ (**1a** ↔ **1a′** and **1d** ↔ **1d′**). It is important to note that because energy barriers for these conversions lie far below the entrance channel, the complexes could convert into each other readily and eventually would predominantly populate in the "classical" states.

3.2. Elimination of H_2. We have extensively surveyed all possible pathways for the loss of H_2 and found that at least one high energy barrier lying above the entrance channel is involved in the mechanisms of direct elimination from two adjacent groups, initial N−H activation, and initial C^β−H activation. Thus they are not important for the product and will not be included in the discussion for simplicity. For details the readers can refer to the Supporting Information (see Figures S2−S6). In the following, we will only discuss the most important dehydrogenation pathways.

These important pathways involve initial C^α−H activation. Calculated PES together with schematic structures involved in the channel is shown in Figure 3. Information about the relevant species is given in Figure S7. Through the respective low-energy routes, encounter complexes **1a**, **1b**, and **1c** could convert to C^α−H insertion species **2** (E_{rel} = −36.6 kcal/mol), which is structurally analogous to the C−H insertion species of Cu^+−methylamine,[33] where the metal locates just above the C−N bond with comparable Cu^+−N and Cu^+−C distances. Starting from adduct **1a**, Co^+ insertion into the closer C−H bond of the adjacent CH_2 group could form species **2**. Transition state $\mathbf{TS_{1a-2}}$ for this possibility is 21.7 kcal/mol lower in energy than that for initial N−H insertion $\mathbf{TS_{1a-S2}}$ (see Figures 3 and S3). This saddle point occurs late along the reaction coordinate. Starting from **1b**, an intrarotation of the Co^+H^3 entity around the axis parallel approximately with the C−C bond could also result in species **2**. This possibility involves transition state $\mathbf{TS_{2-1b}}$ that lies 21.0 kcal/mol below the entrance channel. For complex **1c**, the "bridge" η^2 coordination favors Co^+ insertion into the attached C^α−H bond, giving species **2c**. The relevant transition state $\mathbf{TS_{1c-2c}}$ lies above **1c** and **2c** by 7.7 and 4.8 kcal/mol, respectively. Subsequently, a simultaneous swing of the methyl and Co^+H groups that stabilize the system by 9.2 kcal/mol through a nearly energy-free barrier ($\mathbf{TS_{2c-2}}$) could convert **2c** into **2**.

Once species **2** is formed, three different pathways could be followed due to methyl- and amino-H shifts. Along the methyl-H shift pathway, molecular-hydrogen complex **3** is formed by a methyl-H migration onto the metal center. Transition state $\mathbf{TS_{2-3}}$ for this possibility lies 19.9 kcal/mol below the entrance channel. Direct dissociation of **3** would account for dehydrogenation product **1**−**1**. The new species **3** and the resulting product **1**−**1** are quite stable (E_{rel} = −50.9 and −36.4 kcal/mol, respectively). For the amino-H shift mechanism, two different pathways could be followed. The first pathway to form molecular-hydrogen complex **4′** involves transition state $\mathbf{TS_{2-4'}}$, lying 5.9 kcal/mol below the entrance channel. Decomposition of **4′** would give product **1**−**2** with an overall exothermicity of 43.2 kcal/mol. Alternatively, species **2** could experience the other amino-H shift that stabilizes the system by 25.7 kcal/mol to form molecular-hydrogen complex **4**. Transition state $\mathbf{TS_{2-4}}$ for this possibility lies 5.2 kcal/mol below the entrance channel. The dehydroge-

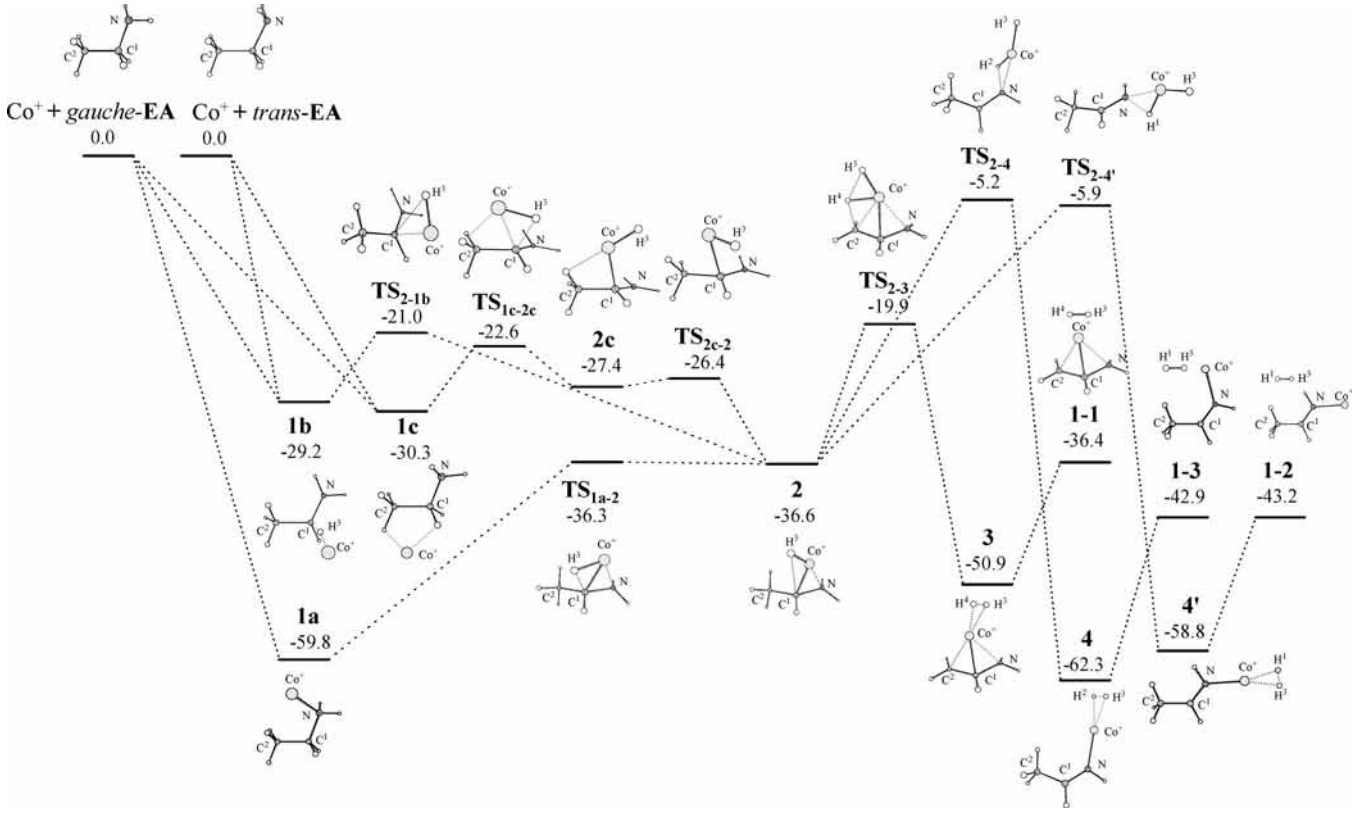

Figure 3. Energy profile for the loss of H_2 through initial $C^{\alpha}-H$ activation. Parameters follow the same notations as in Figure 2.

nation of species **4** would account for product **1**−**3** with an exothermicity of 42.9 kcal/mol for the overall reaction. Note that although the possibilities for producing products **1**−**1**, **1**−**2**, and **1**−**3** through the above-mentioned routes are all energetically favorable, the last two products are consistent with the ICR experimental findings.[14]

3.3. Elimination of CoH. Although the hydride abstraction of Mg^+−amine complexes and methylamine with Cu^+ has been theoretically investigated,[22a,d,33] to understand the effects of both the metal ions and the amines as well as to shed light on the competitions between different product channels, here we also carry out a theoretical study of the hydride abstraction of **EA** with Co^+. Calculated PES together with schematic structures involved in the channel is shown in Figure 4. Information about the relevant species is given in Figure S8. We can find this channel arises from complexes **1a**, **1a′**, **1b**, and **1c**. Analogous to the hydride abstraction of methylamine with Cu^+,[33] the hydride abstraction involves a key intermediate (**1b**), which could be formed via (1) direct complexation of Co^+ with **EA**, (2) direct transformation from **1a′** by simple movement of the metal via transition state $\mathbf{TS_{1a'-1b}}$, (3) stepwise process of **1a**→ **2** → **1b** through $C^{\alpha}-H$ activation and subsequent intrarotation of CoH^+ via transition states $\mathbf{TS_{1a-2}}$ and $\mathbf{TS_{2-1b}}$, respectively, (4) direct rearrangement from **1c** through $\mathbf{TS_{1b-1c}}$, (5) stepwise rearrangement of **1c**→ **2c** → **2** → **1b** through transition states $\mathbf{TS_{1c-2c}}$, $\mathbf{TS_{2c-2}}$, and $\mathbf{TS_{2-1b}}$, respectively. Note that all these parallel routes are calculated to be at least 21 kcal/mol lower in energy than the separated reactants, suggesting the preference for formation of the intermediate.

It is expected that the hydride abstraction product should be an asymptote correlated with the associated precursors having a $CH_3CHNH_2^+-CoH$ configuration. However, because their positive charge is mainly located on CoH (see Table 3), intermediates **2**, **2c**, and **1b** should have a configuration of $CH_3CHNH_2-CoH^+$ and would dissociate directly into product **2**−**2** with an appearance energy of 47.2 kcal/mol. Therefore, to form the direct precursors of the hydride abstraction product, charge-transfer (CT) processes should be followed. As shown in Figure 4, two different CT pathways are followed for species **1b** to arrange into the respective precursors of the hydride abstraction product. The first one follows the earlier-reported CT mechanism,[22a,d,33] in which an extensive intrarotation of the CH_3CHNH_2 entity that stabilizes the system by 2.4 kcal/mol would transfer **1b** into **5**. The relevant saddle point ($\mathbf{TS_{1b-5}}$) is only 2.6 kcal/mol higher in energy than **1b**. The new species is featured by a classical N−H···H−M group[22a,d,33] as well as an $imine^+-HM$ configuration as mirrored by the charge on the CoH entity (see Table 3). Nonreactive dissociation of the CH_3CHHNH^+-HCo bond would account for product **2**−**1**, which is exothermic by 13.6 kcal/mol for the overall reaction.

In addition to the above process, it is important to note that a new CT route from **1b** is also identified. When species **1b** is formed, the stretching of the C^1-H^3 bond via transition state $\mathbf{TS_{1b-6}}$ could lead to the formation of species **6**. In the new species, the respective C^1-C^2 and C^1-N bond lengths are almost identical to those of free $CH_3CHNH_2^+$, and the Co^+-H^3 distance is also close to that in free CoH (see Figure S8). Also, the positive charge in this species locates primarily on CH_3CHNH_2 (0.121 e for CoH; see Table 3). Therefore, the new species also possesses the $CH_3CHNH_2^+-HCo$ configuration as found for **5** in spite of their different structures. Indeed, in contrast to the "classical" N−H···H−M association of **5**, species **6** is featured by a Co−H···C^{α} association with the H−C^{α} distance of 2.216 Å. A general relation between charge distributions and geometries for the $[CH_2NH_2-CuH]^+$ species has been discussed previously.[33] NBO analysis shows that, similar to the situation of $CH_2NH_2^+-CuH$,[33] in species **5** and **6** the C^1 atom does not form any covalent bond with CoH but

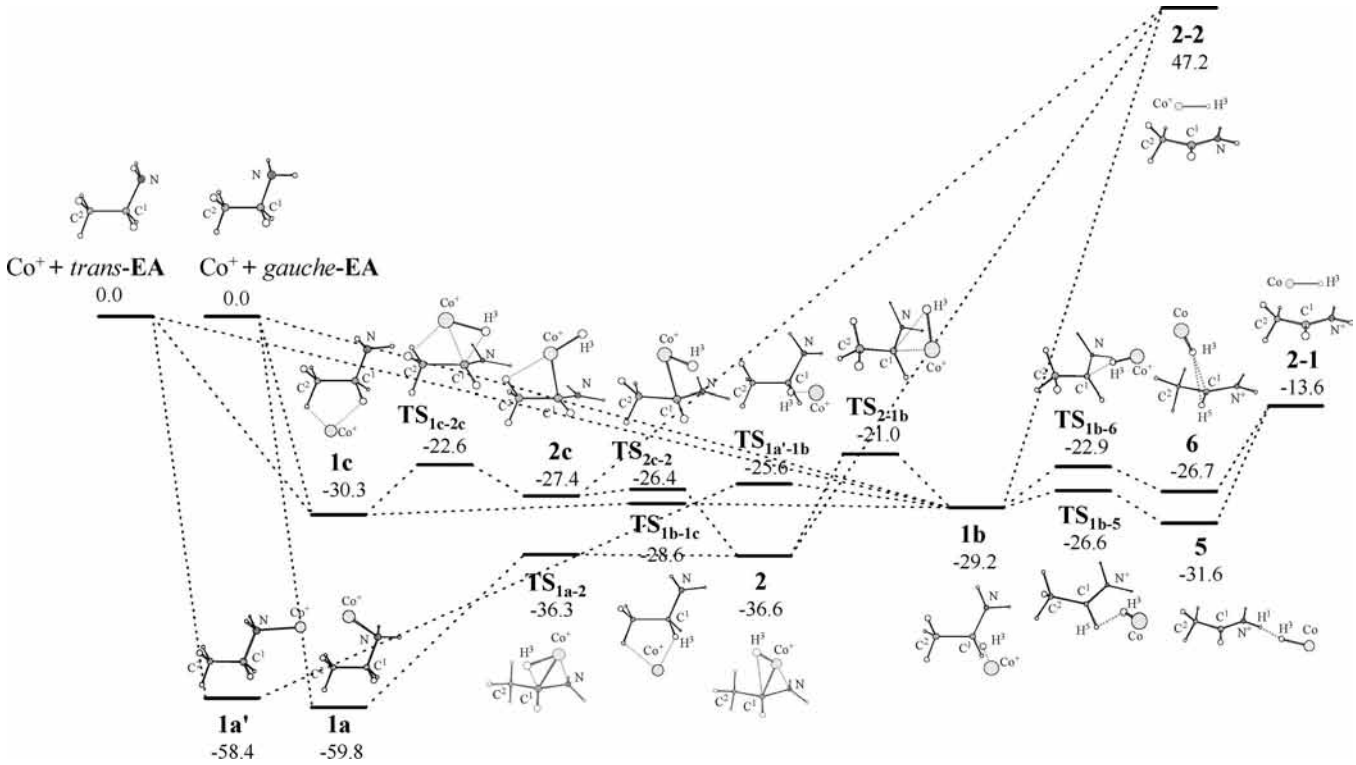

Figure 4. Energy profile for the loss of CoH. Parameters follow the same notations as in Figure 2.

TABLE 3: Calculated Natural Charges on CoH (in e) for Species Involved in the Hydride Abstraction of Ethylamine with Co^+ at the NBO//B3LYP/6-311++G(2df,2pd) Level

species	charges	species	charges
2	0.655	$\mathbf{TS_{1a-2}}$	0.816
2c	0.544	$\mathbf{TS_{1c-2c}}$	0.640
1b	0.671	$\mathbf{TS_{2c-2}}$	0.551
5	0.083	$\mathbf{TS_{1b-1c}}$	0.750
6	0.121	$\mathbf{TS_{1b-5}}$	0.034
		$\mathbf{TS_{1b-6}}$	0.316

forms a π bond with N instead (see Table S3) due to the large C^1-H^3 distance as well as the relatively low ionization energy of CH_3CHNH_2 with respect to CoH.[49,50] The $Co-H\cdots C^\alpha$ association is stabilized by electron donation from $\sigma(Co-H^3)$ to a $\pi^*(C^1-N)$ antibonding orbital (see Table S4). Similar to **5**, species **6** could also account for the hydride abstraction product **2**−**1**.

3.4. Elimination of CH_4. Calculated PES together with schematic structures involved in the channel is shown in Figure 5. Information about the relevant species is given in Figure S9. We can find that encounter complexes **1a** and **1c** could account for the demethanation product. Once encounter complex **1a** is formed, Co^+ insertion into the C−C bond that destabilizes the system by 19.1 kcal/mol would lead to C−C insertion species **7**. This possibility involves saddle point $\mathbf{TS_{1a-7}}$ lying 24.3 kcal/mol below the entrance channel. The subsequent process that Co^+ acts as a "carrier" to ferry the methylene H atom to the methyl group constitutes the rate-determining step of the overall reaction, because the relevant transition state ($\mathbf{TS_{7-8}}$) lies 11.6 kcal/mol above the entrance channel. The resulting minimum **8** is a quite stable methane complex of $H_4C-Co^+CH(NH_2)$ (E_{rel} = −54.8 kcal/mol), in which Co^+ η^2-coordinates to the methane entity as the $COCo^+-CH_4$ complex does.[22c,f] Nonreactive dissociation of the new species would account for **3**−**1**, which is exothermic by 39.4 kcal/mol with respect to the entrance channel.

For the other demethanation pathway, starting from encounter complex **1c**, the metal could also insert into the C−C bond of **EA** giving C−C insertion species **7c**, a nearly isoenergetic structure of its precursor. The transition state for this possibility ($\mathbf{TS_{1c-7c}}$) is 14.3 kcal/mol higher in energy than the above-mentioned C−C activation transition state $\mathbf{TS_{1a-7}}$ or lies 13.3 kcal/mol below the entrance channel. However, this possibility is favorable both dynamically and energetically, because it is expected the complexation process for forming **1c** results in strong excitation of the $H-Co^+-H$ scissor vibration in the complex. The subsequent H shift process from **7c** to **8** is analogous to **7** → **8**; i.e., one of the methylene H's shifts to the methyl C mediated by the metal. However, it is important to note that in this case the energy of the involved transition state ($\mathbf{TS_{7c-8}}$) is relatively low, lying 5.7 kcal/mol below the entrance channel. The forward minimum **8** has been discussed above. Note that this latter demethanation pathway is strictly analogous to the reaction of transition metal ions with alkanes.[43,46–48]

In summary, although two demethanation pathways starting respectively from classical complex **1a** and nonclassical complex **1c** are identified, the latter one is expected to result in the product and the former one is unlikely to be important due to one high energy barrier located along the route.

3.5. Elimination of C_2H_4. Calculated PES together with schematic structures involved in the channel is shown in Figure 6. Information about the relevant species is given in Figure S10. We can find that the reaction could start from encounter complex **1a**, **1a′**, or **1d**. For complexes **1a** and **1a′**, oxidative addition of the metal across the C−N bond could account for intermediates **9** and **9′**; the relevant transition states $\mathbf{TS_{1a-9}}$ and $\mathbf{TS_{1a'-9'}}$ lie 21.2 and 11.9 kcal/mol below the entrance channel, respectively. Both the new minima are featured by the rupture of the C−N bond and the formation of the Co^+-C bond as mirrored by the corresponding bond lengths. Furthermore, the structure of species **9** also favors an agostic interaction between the metal and one (H^4) of the methyl H's, explaining its stability (E_{rel} =

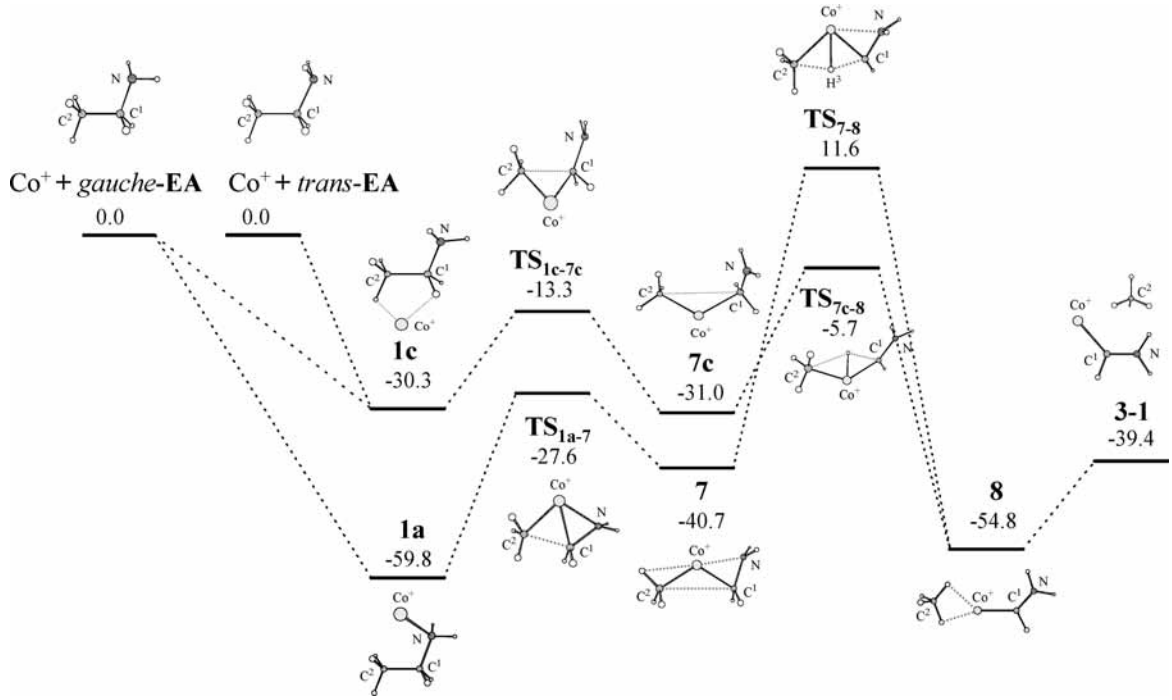

Figure 5. Energy profile for the loss of CH_4. Parameters follow the same notations as in Figure 2.

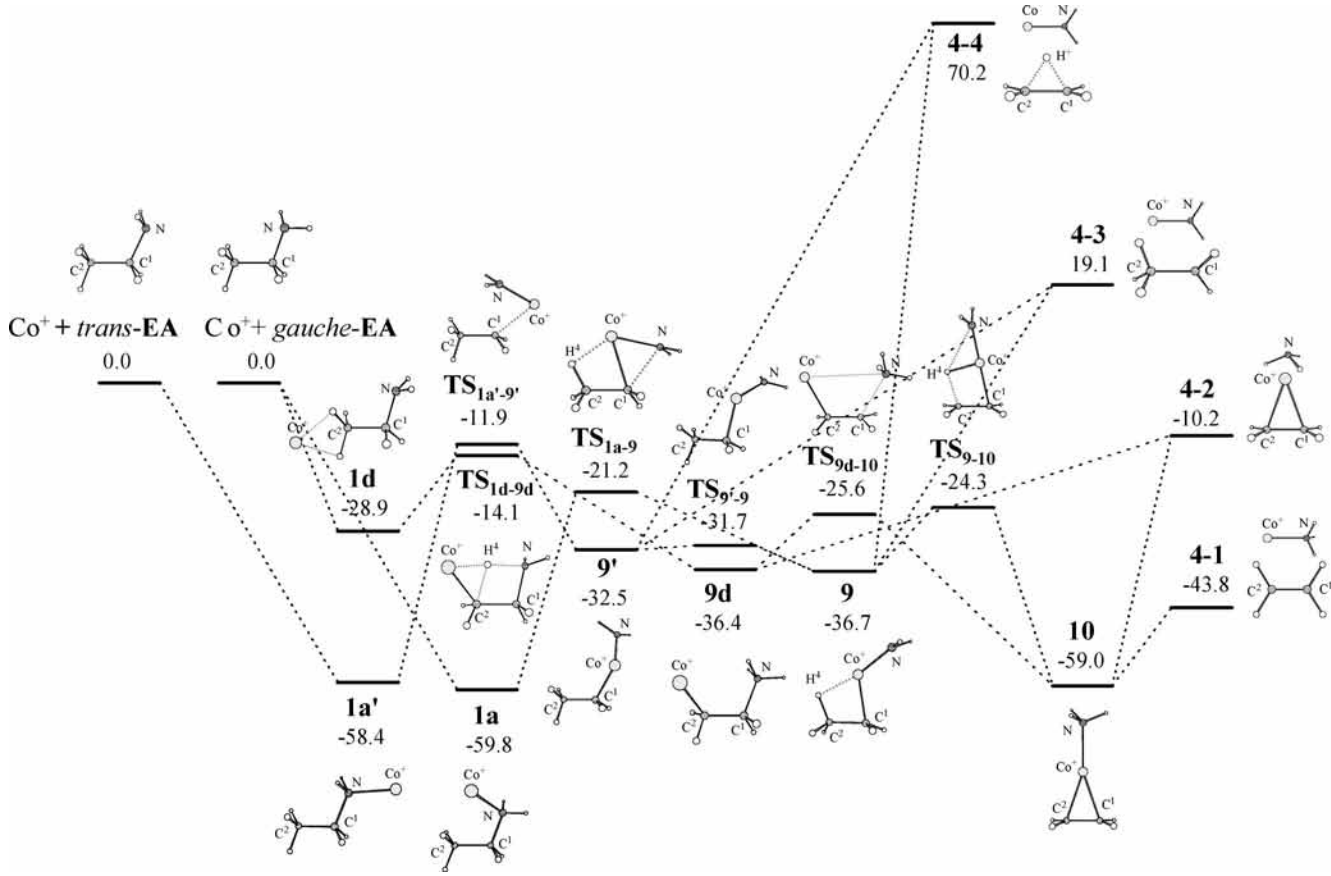

Figure 6. Energy profile for the loss of C_2H_4 and NH_3. Parameters follow the same notations as in Figure 2.

−36.7 kcal/mol) with respect to that of **9′** (E_{rel} = −32.5 kcal/mol). **9** and **9′** each could be followed by three exit channels via direct decompositions and rearrangements. The first two are their direct decompositions into products **4**−**3** and **4**−**4** with the high appearance energies of 19.1 and 70.2 kcal/mol, respectively, in accordance with the experimental results that no such products were observed.[14,15] The last exit of **9′** is the possibility to form the more stable isomer **9** with an energy barrier of only 0.8 kcal/mol (**TS$_{9'-9}$**). For species **9**, the last exit is the concerted, metal mediated shift of the methyl H in the agostic bond to the amino group to form the dicoordinated ammonia−Co^+−ethene complex **10**. This possibility involves transition state **TS$_{9-10}$** lying 24.3 kcal/mol below the entrance channel. Owing to the strong interaction of Co^+ with both

connected ligands, the new species is very stable, lying 59.0 kcal/mol below the entrance channel. Direct dissociations of **10** would account for products **4**−**1** and **4**−**2** with the respective exothermicities of 43.8 and 10.2 kcal/mol. The large exothermicity value of **4**−**1** is consistent with the experimental findings that only this C−N activation product was observed in the metastable dissociation of Co^+-**EA**.[15]

It is interesting to note that a different mechanism could also be experienced for nonclassical complex **1d** to eliminate NH_3 and C_2H_4, i.e., methyl-H migration followed by C−N rupture. In the first step of this pathway, starting from **1d**, the metal oxidative addition accross the coordinated C−H bond on the same side of the amino group makes the shift of the methyl H onto the amino group possible. This possibility involves transition state $\mathbf{TS_{1d\text{-}9d}}$, in which the C^2-H^4 bond has been broken and the new bonds of Co^+-C^2 and $N-H^4$ have been formed. Note that this transition state is 14.1 kcal/mol lower in energy than the entrance channel, suggesting this process is also possible. The resulting new species (**9d**) with a relative energy of −36.4 kcal/mol has a *cis*-$Co^+CH_2CH_2NH_3$ configuration with the C^1-N distance stretched to 1.528 Å (compared to 1.443 Å in **1d**). Direct decomposition of the weakened C^1-N bond of **9d** would produce product **4**−**2**. Alternatively, it could rearrange to species **10**, accounting for final products **4**−**1** and **4**−**2** via transition state $\mathbf{TS_{9d\text{-}10}}$ that lies 25.6 kcal/mol below the entrance channel.

3.6. Comparison with Experimental Results. In this section, we briefly compare our theoretical results with the experimental findings from both ICR and metastable dissociation studies.[14,15] Experimentally, some reactions, such as dehydrogenation, hydride abstraction, demethanation, and loss of other hydrocarbon neutrals, account for gas-phase chemistry of Co^+ with primary amines. Several main points can be summarized for the reactions of Co^+ with **EA** and other amines. First, ICR and metastable dissociation experiments gave not only different product distributions but also different product abundances for the reactions of Co^+ with **EA**. For instance, in the ICR study the products in increasing-abundance sequence were H_2 (15%), CH_4 (26%), and CoH (59%),[14] whereas those were C_2H_4, CoH, and H_2 via metastable dissociation.[15] Second, for the H_2 loss from amines via reaction with Co^+, labeling experiments with $C_2H_5ND_2$ (eliminated HD predominantly) together with other experimental findings in the ICR study let the authors propose a dehydrogenation mechanism of initial N−H insertion followed by α-methylene-H shift, and the resulting product was thus conjectured to be Co^+−imine complex.[14] However, this mechanism was later revised by the "remote functionalization" mechanism for the gas-phase reactions of Co^+−propylamine, because metastable ion decompositions of the Co^+ complexes with a set of *n*-propylamine isotopomers liberated molecular hydrogen originated from the β and γ positions of the propyl chain.[13a]Third, because in the ICR experiment hydride abstraction with Co^+ occurred in the case of triethylamine (which contains no amine-hydrogen atom) and methylamine (which contains only $C^\alpha-H$ atom) but not for *tert*-butylamine (which has no $C^\alpha-H$ atom), this process was predicted to be from the α-methylene group.[14] Metastable ion decompositions of the D-labeled *n*-propylamine complexes with Co^+ and Ni^+ confirmed this point.[13a] Fourth, in the ICR experiment, the loss of small alkanes and alkenes from primary amines via reactions with Co^+ was conjectured to proceed through initial insertion of the metal into C−C bonds, which parallels the reactions observed for alkanes with similar skeletal structures.[14] However, D-labeling experiments suggested that the ethene loss in the metastable dissociation of Co^+−*n*-propylamine can be described in terms of the "remote functionalization" concept.[13a] Last, the products associated with C−N activation were not observed for the Co^+ + primary amine reactions in the ICR experiments,[14] whereas loss of C_2H_4 was indeed observed as a minor product from the metastable dissociation of the Co^+-**EA** complex.[15]

From Figures S2, S3, S5, and 3, we can find that although quite a large number of dehydrogenation pathways are theoretically identified, the pathways involving $C^\alpha-H$ activation followed respectively by amino-H (**1a**, **1b**, **1c** → **2** → **4′** → **1**−**2** and **1a**, **1b**, **1c** → **2** → **4** → **1**−**3**) and methyl-H (**1a**, **1b**, **1c** → **2** → **3** → **1**−**1**) shifts seem to be more possible, because only along these pathways are all the transition states and minima located below the entrance channel (see Figure 3). Note that the structures of products **1**−**2** and **1**−**3** are consistent with the dehydrogenation product observed in the ICR experiment.[14] This reaction mechanism is contrary to the mechanism proposed by Radecki and Allison, i.e., Co^+ insertion into N−H bond followed by α-methylene H shift.[14] The latter mechanism (**1a′** → **S2′** → **4′** → **1**−**2**) is not so energetically favorable (see Figure S3).

Distributions and relative intensities of the final products are determined by several factors, such as experimental methods, reaction energies, and competitions between different product channels. A complete description of the experimental observations would require dynamical calculations that are out of the scope of this article. However, the different experimental methods employed can still give some hints for our discussion. For instance, all the encounter complexes (including "classical" and "nonclassical") can serve as the sources of the products observed in the ICR experiment, whereas metastable decompositions involve only the classical complexes (**1a** and **1a′**), because, as discussed above, before the dissociations take place most of the nonclassical complexes (**1b**, **1c**, **1d**, and **1d′**) should be quenched to the more stable classical forms. Taking into account these facts and with the help of the present calculated results, several qualitative points can be gained. First, the fact that only nonclassical complex **1c** accounts for the loss of methane (**1c** → **7c** → **8** → **3**−**1**; see Figure 5) explains why the product was not observed in the MI spectrum[15] but indeed formed in the ICR experiment.[14] Second, a large number of encounter complexes (**1a**, **1a′**, **1b**, and **1c**) implying the hydride abstraction (see Figure 4) explains why in the ICR experiment the product was the most abundant[14] and it fell to the intermediate abundance in the MI spectrum,[15] because in the latter case encounter complexes **1b** and **1c**, which are expected to be important sources for the hydride abstraction, have been depopulated to a large extent before the metastable decompositions taking place. Third, at this time it is unable to give an explicit explanation of the fact that no product corresponding to C−N activation was observed in the ICR experiment,[14] because the pathways associated with this product channel are also quite low in energy (see Figure 6). A plausible explanation may be that the product from encounter complexes **1a**, **1a′**, and **1d** was suppressed by the loss of H_2 and CoH. Indeed, the relatively low peak associated with the C_2H_4 loss product in the MI spectrum[15] suggests complexes **1a** and **1a′** imply predominantly loss of H_2 and CoH. It is interesting to note that the preference of the H_2 and CoH loss to the C_2H_4 loss is consistent with the energies of initial bond activation barriers for the corresponding product channels (23.5 kcal/mol for initial $C^\alpha-H$ activation vs 38.6−46.5 kcal/mol for initial C−N activation; see Figures 3, 4, and 6). Last, the nonclassical

associations of amines with Co^+ are the reason amine reactions closely paralleled alkane reactions in the ICR experiment.[14]

4. Conclusion

This theoretical work has advanced the earlier experimental studies on the gas-phase reactions of Co^+ with ethylamine and shed new light on the reaction mechanisms of transition metal ion with primary amines. We can now conclude by summarizing a number of main points below.

(1) In addition to the classical N attached complexes, various nonclassical complexes could be formed due to attacks of Co^+ at different ethyl H(s) of either *gauche*- or *trans*-ethylamine. Binding energies for the classical complexes are much higher (~59 kcal/mol) and the nonclassical ones have complexation energies close to those of Co^+ complexes with small alkanes (~29 kcal/mol). These encounter complexes could transfer into each other and have the tendency to convert to the classical forms. Both the classical and nonclassical complexes could account for products observed experimentally for the gas-phase reactions of Co^+ with ethylamine.

(2) The loss of H_2 involves not only the classical complex with *gauche*-ethylamine (**1a**) but also the nonclassical complexes of either *gauche*- or *trans*-ethylamine (i.e., the η^1 methylene-H attached complex (**1b**) and the complex with the metal bound to two H atoms from the different carbons of ethylamine (**1c**)). This product channel could take place via Co^+ insertion into a $C^{\alpha}-H$ bond followed respectively by amino- and methyl-H shifts, and products from the former H-shift pathways are consistent with experimental findings. The earlier-proposed N−H activation−α-methylene H shift mechanism is unlikely to be important.

(3) The loss of CoH is α-hydride abstraction. This channel involves the same nonclassical complexes as for the H_2 loss. In addition, classical complexes with both *gauche*- and *trans*-ethylamines (**1a** and **1a′**) also imply this product. **1b** is the key intermediate for this product channel, which is followed by two parallel charge-transfer processes giving the product.

(4) Demethanation occurs only from nonclassical complex **1c**, followed by a pathway strictly analogous to small alkane reactions, i.e., C−C activation and subsequent methylene-H shift.

(5) The loss of C_2H_4 arises from Co^+ insertion into the polar C−N bond starting from classical complexes **1a** and **1a′** followed by a subsequent β-H shift. In addition, Initial $C^{\beta}-H$ activation from the nonclassical methyl-H attached complex of Co^+−*gauche*-ethylamine (**1d**) also implies this product. The low yield of this product is consistent with a relatively high energy barrier for the polar C−N activation (with respect to that for $C^{\alpha}-H$ activation).

(6) Different distributions and relative intensities of the final products observed in ICR and metastable dissociation experiments can be attributed predominantly to the different methods used; i.e., the metastable dissociation of Co^+−ethylamine involves predominantly the classical complexes, whereas in the ICR experiment both the classical and nonclassical complexes could contribute to the products. The reactions of the nonclassical complexes closely parallel with alkane reactions with Co^+ and can serve as the reason primary amines exhibit gas-phase chemistry parallel with alkanes.

Acknowledgment. This work was supported by SRF for ROCS and NCET-05-0608 of MOE, PRC, National Natural Science Foundation of China (20476061), Natural Science Foundation of Shandong Province, PRC (Y2006B35), and State Key Basic Research Program of PRC (2006CB202505).

Supporting Information Available: Optimized structures as well as selected structural parameters for the transition states involved in the conversions between Co^+−ethylamine complexes; optimized geometries and selected structural parameters for all the intermediates, saddle points and products for the loss of H_2, CoH, CH_4, and C_2H_4; energy profiles for the loss of H_2 via direct mechanisms from two adjacent groups, initial N−H activation, and initial $C^{\beta}-H$ activation; calibration; calculated total energies, zero-point energies, and values of $\langle S^2 \rangle$ for all the relevant species; NBO results for the $[CoH + CH_3CHNH_2]^+$ species. This material is available free of charge via the Internet at http://pubs.acs.org.

References and Notes

(1) Burnier, R. C.; Carlin, T. J.; Reents, J. W. D.; Cody, R. B.; Lengel, R. K.; Freiser, B. S. *J. Am. Chem. Soc.* **1979**, *101*, 7127.
(2) Lombarski, M.; Allison, J. *Int. J. Mass. Spectrom. Ion Phys.* **1983**, *49*, 281.
(3) Buckner, S. W.; Freiser, B. S. *J. Am. Chem. Soc.* **1987**, *109*, 4715.
(4) (a) Sigsworth, S. W.; Keesee, R. G.; Castleman, J. A. W. *J. Am. Chem. Soc.* **1988**, *110*, 6682. (b) Sigsworth, S. W.; Castleman, J. A. W. *J. Am. Chem. Soc.* **1989**, *111*, 3566.
(5) (a) Eller, K.; Schwarz, H. *Organometallics* **1989**, *8*, 1820. (b) Eller, K.; Schwarz, H. *Chem. Rev.* **1991**, *91*, 1121.
(6) (a) Chen, Y. M.; Clemmer, D. E.; Armentrout, P. B. *J. Chem. Phys.* **1991**, *95*, 1228. (b) Chen, Y. M.; Clemmer, D. E.; Armentrout, P. B. *J. Chem. Phys.* **1993**, *98*, 4929.
(7) Chen, L. Z.; Miller, J. M. *J. Am. Soc. Mass Spectrom.* **1992**, *3*, 451.
(8) Armentrout, P. B.; Kickel, B. L. In *Organometallic Ion Chemistry*; Freiser, B. S., Ed., Kluwer: Dordrecht, The Netherlands, 1995, p 1.
(9) Luna, A.; Amekraz, B.; Morizur, J.-P.; Tortajada, J.; Mó, O.; Yáñez, M. *J. Phys. Chem. A* **1997**, *101*, 5931.
(10) Aribi, H. E.; Rodriquez, C. F.; Shoeib, T.; Ling, Y.; Hopkinson, A. C.; Siu, K. W. M. *J. Phys. Chem. A* **2002**, *106*, 8798.
(11) (a) Alcamí, M.; Luna, A.; Mó, O.; Yáñez, M.; Tortajada, J.; Amekraz, B. *Chem. Eur. J.* **2004**, *10*, 2927. (b) Alcamí, M.; Mó, O.; Yáñez, M. *Mass Spectrom. Rev.* **2001**, *20*, 195.
(12) Babinect, S. J.; Allison, J. *J. Am. Chem. Soc.* **1984**, *106*, 7718.
(13) (a) Karrass, S.; Priisse, T.; Eller, K.; Scbwarz, H. *J. Am. Chem. Soc.* **1989**, *111*, 9018. (b) Karrass, S.; Scbwarz, H. *Organometallics* **1990**, *9*, 2034. (c) Karrass, S.; Scbwarz, H. *Organometallics.* **1990**, *9*, 2409. (d) Karrass, S.; Stöckigt, D.; Schröder, D.; Schwarz, H. *Organometallics.* **1993**, *12*, 1449.
(14) Radecki, B. D.; Allison, J. *J. Am. Chem. Soc.* **1984**, *106*, 946.
(15) Chen, L. Z.; Miller, J. M. *Inorg. Chem.* **1992**, *31*, 4029.
(16) Clemmer, D. E.; Armentrout, P. B. *J. Phys. Chem.* **1991**, *95*, 3084.
(17) (a) Holthausen, M. C.; Fiedler, A.; Schwarz, H.; Koch, W. *J. Phys. Chem.* **1996**, *100*, 6236. (b) Holthausen, M. C.; Koch, W. *J. Am. Chem. Soc.* **1996**, *118*, 9932.
(18) Hoyau, S.; Ohanessian, G. *Chem. Phys. Lett.* **1997**, *280*, 266.
(19) (a) Luna, A.; Amekraz, B.; Tortajada, J. *Chem. Phys. Lett.* **1997**, *266*, 31. (b) Luna, A.; Alcamí, M.; Mó, O.; Yáñez, M. *Int. J. Mass. Spectrom.* **2000**, *201*, 215. (c) Luna, A.; Alcamí, M.; Mó, O.; Yáñez, M. *Chem. Phys. Lett.* **2000**, *320*, 129.
(20) Shiota, Y.; Yoshizawa, K. *J. Am. Chem. Soc.* **2000**, *122*, 12317.
(21) Fedorov, D. G.; Gordon, M. S. *J. Phys. Chem. A* **2000**, *104*, 2253.
(22) (a) Guo, W. Y.; Lu, X. Q.; Hu, S. Q.; Yang, S. H. *Chem. Phys. Lett.* **2003**, *381*, 109. (b) Liu, H. C.; Hu, Y. H.; Yang, S. H.; Guo, W. Y.; Lu, X. Q.; Zhao, L. M. *Chem. Eur. J.* **2005**, *11*, 6392. (c) Zhao, L. M.; Zhang, R. R.; Guo, W. Y.; Wu, S. J.; Lu, X. Q. *Chem. Phys. Lett.* **2005**, *414*, 28. (d) Guo, W. Y.; Yuan, T.; Chen, X. F.; Zhao, L. M.; Lu, X. Q.; Wu, S. J. *J. Mol. Struc (THEOCHEM)* **2006**, *764*, 177. (e) Chen, X. F.; Guo, W. Y.; Zhao, L. M.; Fu, Q. T. *Chem. Phys. Lett.* **2006**, *432*, 27. (f) Zhao, L. M.; Zhang, R. R.; Guo, W. Y.; Wu, S. J.; Lu, X. Q. *ChemPhysChem* **2006**, *7*, 1345. (g) Chen, X. F.; Guo, W. Y.; Zhao, L. M.; Fu, Q. T.; Ma, Y. *J. Phys. Chem. A* **2007**, *111*, 3566.
(23) Galiano, L.; Alcamí, M.; Mó, O.; Yáñez, M. *J. Phys. Chem. A* **2002**, *106*, 9306.
(24) Zhang, D. J.; Liu, C. B.; Bi, S. W.; Yuan, S. L. *Chem. Eur. J.* **2003**, *9*, 484.
(25) Zhang, Q.; Bowers, M. T. *J. Phys. Chem. A* **2004**, *108*, 9755.
(26) Lee, C. T.; Yang, W. T.; Parr, R. G. *Phys. Rev B* **1988**, *37*, 785.
(27) Salahub, D. R.; Zerner, M. C. *The Challenge of d and f Electrons*; American Chemical Society: Washington, DC, 1989.

(28) Parr, R. G.; Yang, W. *Density Functional Theory of Atoms and Molecules*; Oxford University Press: Oxford, U.K., 1989.

(29) Labanowski, J. K.; Andzelm, J. W. *Density Functional Methods in Chemistry*; Springer: Berlin, 1991.

(30) Becke, A. D. *J. Chem. Phys.* **1993**, *98*, 1372.

(31) Alcamí, M.; Luna, A.; Mó, O.; Yáñez, M. *J. Phys. Chem. A* **2004**, *108*, 8367.

(32) Ma, Y.; Guo, W. Y.; Zhao, L. M.; Hu, S. Q.; Zhang, J.; Fu, Q. T.; Chen, X. F. *J. Phys. Chem. A* **2007**, *111*, 6208.

(33) Lu, X. Q.; Guo, W. Y.; Zhao, L. M.; Chen, X. F.; Fu, Q. T.; Ma, Y. *J. Organomet. Chem.* **2007**, *692*, 3796.

(34) Becke, A. D. *J. Chem. Phys.* **1993**, *98*, 5648.

(35) Miehlich, B.; Savin, A.; Stoll, H.; Preuss, H. *Chem. Phys. Lett.* **1989**, *157*, 200.

(36) (a) Zeroka, D.; Jensen, J. O.; Samuels, A. C. *J. Phys. Chem. A* **1998**, *102*, 6571. (b) Zeroka, D.; Jensen, J. O.; Samuels, A. C. *J. Mol. Struct. (THEOCHEM)* **1999**, *465*, 119.

(37) (a) Gonzalez, C.; Schlegel, H. B. *J. Chem. Phys.* **1989**, *90*, 2154. (b) Gonzalez, C.; Schlegel, H. B. *J. Phys. Chem.* **1990**, *94*, 5523.

(38) (a) Gräfenstein, J.; Hjerpe, A. M.; Kraka, E.; Cremer, D. *J. Phys. Chem. A* **2000**, *104*, 1748. (b) Gräfenstein, J.; Cremer, D. *J. Mol. Phys.* **2001**, *99*, 981.

(39) Bauernschmitt, R.; Ahlrichs, R. *J. Chem. Phys.* **1996**, *104*, 9047.

(40) Frisch, M. J.; Trucks, G. W.; Schlegel, H. B.; Scuseria, G. E.; Robb, M. A.; Cheeseman, J. R. ; Montgomery, J. A., Jr.; Vreven, T.; Kudin, K. N. ; Burant, J. C.; Millam, J. M.; Iyengar, S. S.; Tomasi, J.; Barone, V.; Mennucci, B.; Cossi, M.; Scalmani, G.; Rega, N.; Petersson, G. A.; Nakatsuji, H.; Hada, M.; Ehara, M.; Toyota, K.; Fukuda, R.; Hasegawa, J.; Ishida, M.; Nakajima, T.; Honda, Y.; Kitao, O.; Nakai, H.; Klene, M.; Li, X.; Knox, J. E.; Hratchian, H. P.; Cross, J. B.; Adamo, C.; Jaramillo, J.; Gomperts, R.; Stratmann, R. E.; Yazyev, O.; Austin, A. J.; Cammi, R.; Pomelli, C.; Ochterski, J. W.; Ayala, P. Y.; Morokuma, K.; Voth, G. A.; Salvador, P.; Dannenberg, J. J.; Zakrzewski, V. G.; Dapprich, S.; Daniels, A. D.; Strain, M. C.; Farkas, O.; Malick, D. K.; Rabuck, A. D.; Raghavachari, K.; Foresman, J. B.; Ortiz, J. V.; Cui, Q.; Baboul, A. G.; Clifford, S.; Cioslowski, J.; Stefanov, B. B.; Liu, G.; Liashenko, A.; Piskorz, P.; Komaromi, I.; Martin, R. L.; Fox, D. J.; Keith, T.; Al-Laham, M. A.; Peng, C. Y.; Nanayakkara, A.; Challacombe, M.; Gill, P. M. W.; Johnson, B.; Chen, W.; Wong, M. W.; Gonzalez, C.; Pople, J. A. *Gaussian 03*, revision B.05; Gaussian, Inc.: Pittsburgh, PA, 2003.

(41) Glendening, E. D.; Badenhoop, J. K.; Reed, A. E.; Carpenter, J. E.; Bohmann, J. A.; Morales, C. M.; Weinhold, F. *NBO50*; Theoretical Chemistry Institute, University of Wisconsin, Madison, WI, 2001.

(42) Perry, J. K.; Ohanessian, G.; Goddard, W. A., III *J. Phys. Chem.* **1993**, *97*, 5238.

(43) Holthausen, M. C.; Koch, W. *J. Am. Chem. Soc.* **1996**, *118*, 9932.

(44) (a) Haynes, C. L.; Fisher, E. R.; Armentrout, P. B. *J. Am. Chem. Soc.* **1996**, *118*, 3269. (b) Haynes, C. L.; Fisher, E. R.; Armentrout, P. B. *J. Phys. Chem.* **1996**, *100*, 18300.

(45) Hendrickx, M.; Ceulemans, M.; Vanquickenbome, L. *Chem. Phys. Lett.* **1996**, *257*, 8.

(46) Fedorov, D. G.; Gordon, M. S. *J. Phys. Chem. A* **2000**, *104*, 2253.

(47) Yi, S. S.; Reichert, E. L.; Holthausen, M. C.; Koch, W.; Weisshaar, J. C. *Chem. Eur. J.* **2000**, *6*, 2232.

(48) Reichert, E. L.; Weisshaar, J. C. *J. Phys. Chem. A* **2002**, *106*, 5563.

(49) Burkey, T. J.; Castelhano, A. L.; Griller, D.; Lossing, F. P. *J. Am. Chem. Soc.* **1983**, *105*, 4701.

(50) Kickel, B. L.; Armentrout, P. B. *J. Am. Chem. Soc.* **1995**, *117*, 764.

JP801653T